Estuarine, Coastal and Shelf Science 296 (2024) 108589

Contents lists available at ScienceDirect

Estuarine, Coastal and Shelf Science

journal homepage: www.elsevier.com/locate/ecss

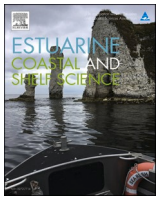

The birth of backbarrier marshes in Culatra Island (Ria Formosa, South Portugal)

Katerina Kombiadou *, A. Rita Carrasco, Susana Costas, Margarida Ramires, Ana Matias

Centre for Marine and Environmental Research (CIMA) / Aquatic Research Network (ARNET), University of Algarve, Campus of Gambelas, 8005-139 Faro, Portugal

ARTICLE INFO

Keywords:
Barrier islands
Salt marshes
Seagrass
Tidal flats
Colonisation lag
Sediment distribution

ABSTRACT

The rapid elongation of Culatra Island, a sandy barrier in the Ria Formosa chain (S. Portugal), since the mid-1940s led to the formation of three new embayments in its backbarrier that were gradually colonised by halophytic vegetation. This provided a rare opportunity to collect information and data on the very early stages of backbarrier marsh plant establishment and evolution. Sediment (surface and subsurface) sampling in two of the recently formed bays, combined with information extracted from vertical aerial photographs, allowed us to assess modern sedimentation characteristics and vertical accretion rates since the shift from a bare sandflat to a vegetated marsh platform. Present-day topography appears largely inherited by overwash or/and inlet-related tidal deposits that provided the necessary sediment pulse for the formation of an intertidal sandy substrate, suitable for colonisation. The variability in accretion rates, noted even within the same embayment, as well as the differences in accretion balance with similarly young backbarrier marshes, highlight the importance of local conditions (sediment import, distance to creeks and marsh edge, storm frequency and intensity) to marsh build-up, even during the very early stages. Variable accretion rates were also identified over intertidal seagrass patches, indicating similar influences. Organic deposition rates were very low in all vegetated intertidal habitats, indicating the dominance of mineral deposition to the vertical growth. A lag, ranging from roughly 10–30 years, was observed between the formation of the intertidal sandy platform and plant establishment in all embayments. The different timescales in the observed lag are likely linked to differences in hydrodynamic conditions, promoted by the embayment morphology (opening width). The lowest lag was observed in protected embayments, which could reflect a 'typical' delay for plant establishment in the system, while the highest lag was associated with higher energy backbarrier environments.

1. Introduction

Saltmarshes are unique coastal habitats of high ecologic and economic value that offer a plethora of important contributions, such as provision of detritus and nutrients to the coastal ocean, nursery grounds of shellfish and finfish, attenuation of storm surges and waves, pollutant assimilation (FitzGerald and Hughes, 2021) and carbon sequestration and storage (Sousa et al., 2017). At the same time, the complex interactions between biological, physical and morphodynamic processes that control their evolution at different timescales make them prime examples of ecological and geomorphological synergy (Belliard et al., 2017). Even though these ecosystems are considered effective as sediment sinks, the nature of this sediment sink function varies markedly between systems (French, 2019), with accretion and evolution depending on several factors, such as sediment availability, plant species and density, salt marsh platform elevation and local hydrodynamics (Pratolongo et al., 2019). Evidence of nonlinear marsh elevation adjustment to accelerating sea levels indicates that increased losses to subsidence can constrain elevation gains (Saintilan et al., 2022). Due to the complexity of interactions and processes and the underlying uncertainties, resolving all sediment fluxes in a marsh still remains a challenge to be addressed and one that is critical to its future resilience (Fagherazzi et al., 2020).

Backbarrier marshes, developing at the lee of barrier islands and spits, are a marsh landform type with distinct geomorphological settings and interactions, typically characterised by coarser sediment of marine origin and potentially high dynamism (Carrasco et al., 2008). There is no clear relationship between tidal range and backbarrier marsh growth, indicating that other factors (e.g., elevation, suspended sediment, frequency and duration of tidal flooding, peat decomposition, and potential sediment delivery via storm surge, edge erosion or ice rafting) may

* Corresponding author.
E-mail address: akompiadou@ualg.pt (K. Kombiadou).

https://doi.org/10.1016/j.ecss.2023.108589
Received 19 July 2023; Received in revised form 24 November 2023; Accepted 5 December 2023
Available online 9 December 2023

Abbreviations

HM	High Marsh
LiM	*Limoniastrum monopetalum*
LM	Low Marsh
SaR	*Salicornia ramossisima*
SM	Salt Marsh
SpM	*Spartina maritima*
TF	Tidal Flat
ZoM	*Zostera marina*
ZoN	*Zostera noltei*

determine vertical build-up (FitzGerald and Hughes, 2019). Global data collected and analysed by Ouyang et al. (2022) support that backbarrier marshes have the lowest accretion rates among tidal marsh geomorphological categories (e.g., fluvial, transitional and bluff-toe marshes showed higher rates by 1.6–1.8), mainly due to low sediment availability. Even though global estimates might be of little use in terms of transferability and applicability in specific sites, this could still signify a higher vulnerability of backbarrier marshes to rising sea levels compared to other marsh types. Aside from the various ecosystem services attributed to salt marshes, backbarrier marshes also contribute significantly to the resilience of the barrier fronting it (Kombiadou et al., 2019a, 2020), providing stabilisation and reducing landward migration rates (Hein et al., 2021; Walters et al., 2014). The resilience of the marsh-barrier unit is important beyond the scale of the unit itself, as potential perturbations (i.e., drowning) are likely to cascade to dependent systems, such as lagoon marshes located at their lee.

Understanding the dynamics controlling change in backbarrier marshes is essential for assessing their ability to persist under changing environmental conditions, with the time aspect—how fast they form and what is their rate of change in position and morphology—being an important part of this understanding (Bartholdy et al., 2018). The main mechanism promoting the onset of backbarrier salt marsh growth is the introduction of new intertidal sand deposits at the lagoon side of barriers, like washovers and/or flood-tidal deltas (Carrasco et al., 2008; Matias et al., 2008; Rodriguez and McKee, 2021). The origin and geomorphological development of salt marshes can be rapid (e.g., less than 20 years; Carrasco et al. (2008)) in circumstances such as the creation of a relatively sheltered sandflat or mudflat from which a salt marsh could build vertically. This, for example, can be the result of the retreat of a major tidal channel away from a coast or the completion of a new terminal hook at the downdrift end of a barrier island or spit (Allen, 2000). After establishment, tidal marshes accrete vertically by accumulating organic matter mostly from in-situ belowground plant production and by enhancing mineral sedimentation; the latter is the primary factor controlling accretionary process during the juvenile stage of marsh growth, while accretion in well-established marshes is predominantly influenced by plant growth (Boyd and Sommerfield, 2016). There is evidence, however, that as the marsh builds up in height and high-marsh conditions are established, even though the site shifts to an organogenic functioning, relatively coarse sedimentation at the surface of the backbarrier marsh can still be a critical factor for maintaining accretion rates (Goslin et al., 2022).

The relatively young backbarrier marshes of Culatra Island (Ria Formosa, South Portugal) are used to study backbarrier marsh genesis and early evolution through traditional methods, like mapping from aerial photos and surface and subsurface sediment analysis. More specifically, the work aims to: a) identify present-day topography, plant zonation and recent sedimentation; b) assess long-term backbarrier marsh dynamics in terms of horizontal expansion, vertical growth and sediment composition since plant establishment; and c) identify the main controls, phases and related timescales during the early stages of backbarrier marsh development.

2. Study area

2.1. Location and characteristics

The study focuses on Culatra Island, located at the east flank of the Ria Formosa barrier system (Fig. 1). The barrier chain harbours the most important wetland in South Portugal, declared a Natural Park since 1987 and protected under the Ramsar convention and the EU Natura 2000 network. The most recent (2014) mapping of intertidal habitats in Ria Formosa indicates a total extent of 2957.6 ha of salt marshes and 1285.6 ha of seagrasses within the lagoon (Carrasco et al., 2021) and 495.2 ha of backbarrier marshes in the 7 barriers of the system (Kombiadou et al., 2019b). Backbarrier marshes presently develop in four embayments in the lagoon side of Culatra, hereon referred to as Culatra 1 to 4 (numbering from west to east, as shown in Fig. 1c). Even though they represent a small portion of the total area of backbarrier marsh in the system (3.1%, versus 29.6% in neighbouring Armona Island; Fig. 1), these are rare instances of marshes having been formed in the very recent past (50–60 years).

Culatra has been elongating alongshore since the middle of the 20th century, process that was triggered by the change in tidal prism balance within the lagoon after the artificial stabilisation of the updrift Faro-Olhão Inlet (opened in 1929, jetty stabilisation concluded in 1955; Vila-Concejo et al. (2002)). Pacheco et al. (2011) estimated that 75% of the tidal prism of downdrift Armona Inlet (Fig. 1), a natural and non-migrating inlet, which was the main inlet of the lagoon prior to the stabilisation, was transferred to Faro-Olhão by the early 2000s. After the intervention, the elongation rate of the island was enhanced, leading to a doubling of the island's length between 1952 and 2014 (total increase of 3.2 km; Fig. 1c) and respective narrowing of the Armona Inlet width (Kombiadou et al., 2019b).

The growth was most likely sustained by the pre-existing, extensive, ebb shoals of the Armona Inlet (Pacheco et al., 2011) and took place in the form of recurved spits (Fig. 1b). Three new embayments were formed in-between the spits after the stabilisation (Fig. 1c): Culatra 2 was formed sometime between 1930 and 1941 (Esaguy, 1984), Culatra 3 between 1952 and 1958 and Culatra 4 between 1958 and 1969. Thereon, all three embayments gradually developed perched backbarrier marshes. In terms of plan view geometry, the bay entrance width is 100 m for Culatra 2, 250 m for Culatra 3 and 60 m for Culatra 4. Present-day indentation indexes (ratio of embayment depth to embayment entrance) of Culatra 2, 3 and 4 are 5.2, 0.5 and 1.8, classifying as very highly indented, low indented and medium-high indented, respectively (according to the classification of Bowman et al. (2014)).

2.2. Backbarrier dynamics

Ria Formosa is a mesotidal system, with diurnal astronomical tides and average tidal range of 1.3 m for neap tides and 2.8 m for spring tides, that can reach 3.5 m during equinox, and with no significant wave propagation inside the lagoon (Carrasco et al., 2018). Recent relative mean sea-level rate (SLR) estimates for the Portuguese coast range from 2.1 to 2.5 mm/yr for the western coast (Antunes, 2019; Antunes and Taborda, 2009) to 1.5 ± 0.2 mm/yr for the south coast (Dias and Taborda, 1992) (Cascais and Lagos tide gauge data, respectively; location in Fig. 1a), while there is no significant fluvial influx to the system (Andrade et al., 2004). Subsidence in the area is negligible and the Ria Formosa basin can be considered stable (Lobo et al., 2001).

Faro-Olhão (flood dominated) and Armona (ebb dominated) inlets are highly interconnected, with the residual flow along the Olhão channel (Fig. 1b) mainly directed from the former to the latter (Pacheco et al., 2010). As aforementioned, a large part of the tidal prism captured by Armona Inlet in the 1930s began to transfer to Faro-Olhão, after its stabilisation. Measurements from 2004 to 2007, showed that Faro-Olhão

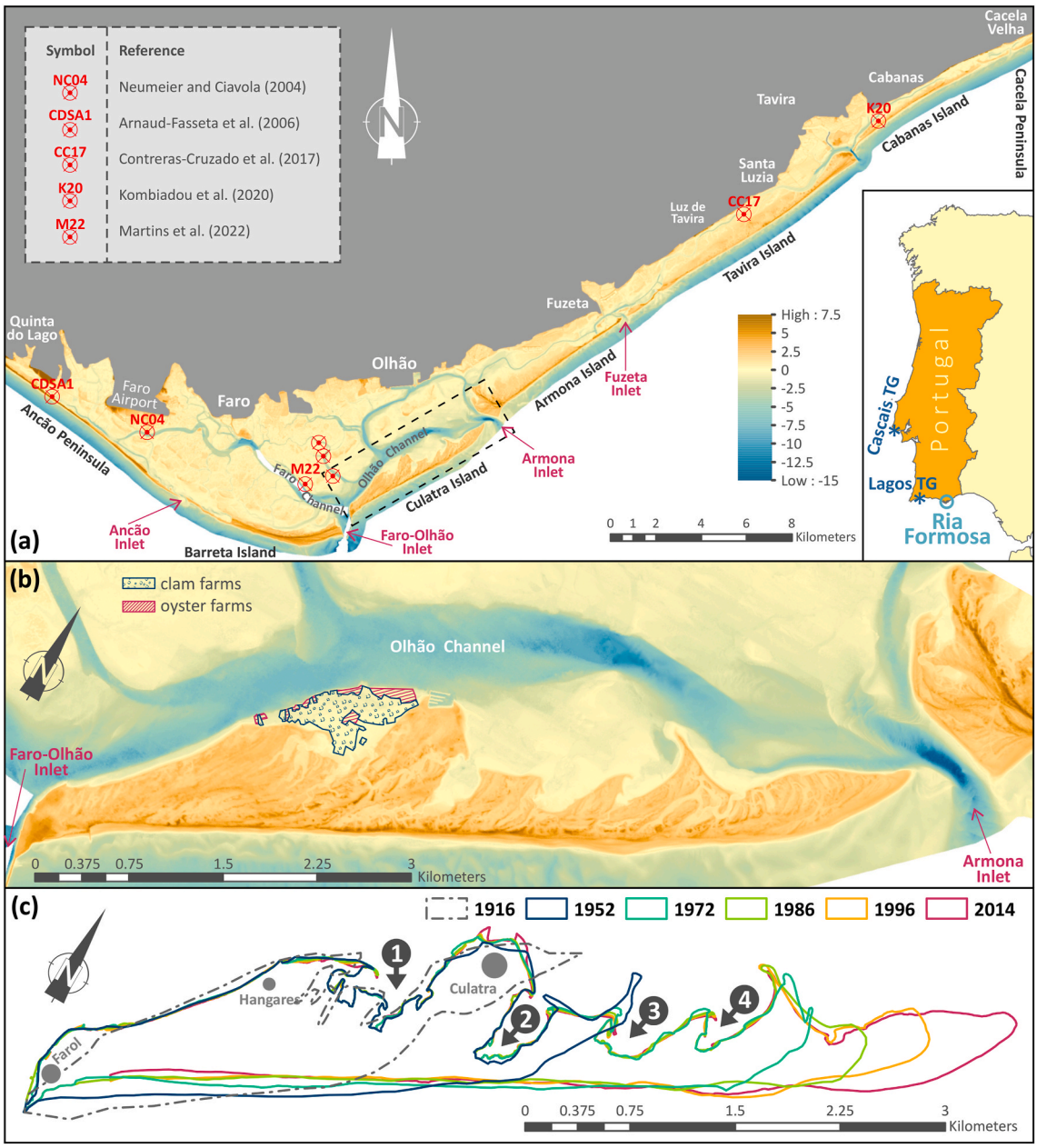

Fig. 1. Digital Terrain Model (DTM; LiDAR, 2011, data from Direção Geral do Territorio) of the Ria Formosa barrier system (a; inset map shows location in Portugal and location of Cascais and Lagos tidal gauges -TG); locations from published works on saltmarsh dynamics are marked on the map (see legend). A zoomed view of the 2011 DTM over Culatra (marked in (a) with dashed polygon; same vertical scale) is given in (b), also showing the extension of licensed oyster and clam farms in the backbarrier (data from 2017; Agência Portuguesa do Ambiente). Selected coastlines of Culatra Island between 1916 and 2014, along with the location of the 4 embayments (1–4) and settlements on the island, are shown in (c; 1916: mapped on the historical map 'Costa Sul de Portugal entre o Cabo de Santa Maria e Vila Real. 1915'; 1952–2014: see Kombiadou et al. (2019b) for ownership of vertical aerial photographs).

Inlet captured 45% of the total neap tidal prism in the system and Armona Inlet captured 40%, with the prism balance for spring tides being at 61% and 23%, respectively (Pacheco et al., 2010). More recent measurements (2011-12) estimate the tidal prism balance at 59–71% for Faro-Olhão and at 37-25% for Armona, for neap to spring tide conditions (Rosa et al., 2019). The shifting tidal prism balance between the inlets on either side of Culatra and its elongation during this period indicates a gradual attenuation of tidal currents along the backbarrier, especially along the eastern part of the island.

The offshore extent of the ebb tidal delta (at around 1.5–1.8 km) and the function of Armona Inlet as a net exporter of sediment were maintained during its narrowing, with the bulk net sediment import taking place through Faro-Olhão (Pacheco et al., 2011; Salles et al., 2005). Regarding surface sediment composition, samples from Armona and Faro Olhão inlets show negligible mud content (0.03 ± 0.2% and 0.3 ± 0.4%) and a dominance of sands (94 ± 8.7% and 86 ± 18.4%), while samples from the Faro channel (Fig. 1a) show slightly higher mud content (3.1 ± 3.6%) (Costas et al., 2018).

2.3. Human occupation and economic activities

There are three settlements on the barrier, Culatra and Hangares that have permanent residents (the former being the main settlement of the island) and Farol that mainly holds touristic lodgings (Fig. 1c). The permanent population is mainly occupied in activities tightly linked to the natural system of Ria Formosa, like fishing and shellfish farming and

gathering (Pacheco et al., 2022). Shellfish (oysters and clams) farming takes place in leased farms in Culatra 1 (5.5 ha allotted to oyster units and 24 ha allotted for clam farming; data from 2017 from Agência Portuguesa do Ambiente; see Fig. 1b), while bivalve collection, activity during which harvesters manually dig and till the sediment, also takes place outside of farms, throughout the intertidal areas of the system. The density of the bivalve harvesters active in the intertidal zones along the backbarrier of Culatra per day is estimated at 54.8 per 100 ha during summer and 27.6 per 100 ha during winter (Cabral et al., 2019). The harvesting process has been linked with direct damage (uprooting or severing plants) and overall severe adverse effects for the *Zostera noltei* meadows of the system (Cabaço et al., 2005).

Aside from traditional activities, the high touristic boom in the Algarve region and the increasing influx to the Ria Formosa region in recent years (i.e., 1991–2002: +35% in Ria Formosa, versus +29% in the Algarve region; Serpa et al. (2005)) may also have increased the environmental pressures to intertidal habitats. In Culatra 2, for example, an increasing number of moored boats within the bay was noted since the mid-1980s, likely due to its proximity to the Culatra settlement and its semi-enclosed morphology. The number of vessels (small boats-SB: 5–6 m length; larger vessels-LV: 7–16 m length) present inside the bay in aerial photographs, typically captured during spring (before the peak of the summer touristic season), shows this trend: 10 (8 SB, 2 LV) in 1986, 19 (4 SB, 15 LV) in 1996, and 86 (42 SB, 44 LV) in 2014. The entrance of the bay was closed off with poles in 2016, impeding access to vessels.

3. Materials and methods

3.1. Mapping and analysis of marsh evolution

The backbarrier marshes of Culatra were mapped on vertical aerial photographs, available between 1952 and 2014 (variable flight intervals; see Kombiadou et al. (2019b) for coverage, resolution, raster ownership and mapping errors). The marshes were mapped as morphological units delimited by: a) the backbarrier coastline at the upper marsh limit (approximately at Mean Highest High-Water; MHHW), and b) the marsh edge boundary at the lagoon side (approximately at Mean Sea Level; MSL). The backbarrier coastline was mapped tracing the upper marsh limit, either by marking the shift to bushy (more rugose, darker) vegetation in areas where the marsh transitioned to dune vegetation, or by marking the upper debris line in areas where the upper marsh bordered with bare sands. The lagoon-side marsh edge was mapped as the boundary between marsh and seagrass vegetation (identified by differences in colour and texture) in areas where the marsh adjoined a vegetated tidal flat, or as the edge of the low-marsh vegetation where it bordered an unvegetated tidal flat (bare sediment).

Long-term (1952–2014) horizontal marsh edge change rates were assessed using the Digital Shoreline Analysis Tool (Thieler et al., 2009) along equidistantly spaced transects (every 4 m), cast vertically along curved reference baselines, drawn so as to cover the extension and form of the mapped marsh-edge lines as much as possible. Horizontal rates were analysed using Weighted Linear Regression (WLR) and setting the total error of each mapped boundary as the uncertainty value (see Kombiadou et al. (2019b) for errors), therefore nudging the regression toward more accurate coastline positions. The marsh area for each embayment was calculated from the shape enclosed within the two mapped boundaries in each flight. Additionally, the 2011 Digital Terrain Model (DTM, in Fig. 1b; horizontal resolution of 2 m and vertical error of 0.15 m) was used to assess the available lateral accommodation space for marsh expansion in the area.

3.2. Field data collection and analysis

Two fieldwork campaigns were conducted to collect surface sediment and core samples in Culatra 2 (June 2017) and Culatra 3 (May 2018). The location of the surface sediment and core sampling stations is given in Fig. 2. Photographs were taken to identify vegetation, while a Trimble R6 RTK-DGPS (Real-Time Kinematic Differential Global Positioning System) was used to collect topographic data. To assess the accuracy of the mapping criteria used for the backbarrier coastline, the upper limit of the marsh (approximately at MHHW; transition to dune vegetation) was mapped using the RTK-DGPS throughout Culatra 2 (Fig. 2) and compared with the coastline mapped on the most recent raster dataset (2014). The distance between them was calculated using the Generate Near Table analysis from the proximity toolset of ArcGIS. Topographic transects were also recorded within the intertidal zone (Fig. A.1), to verify elevational ranges of dominant plants.

In total, seven sediment cores were collected during the campaigns (three from Culatra 2 and four from Culatra 3; Cul2A-2C and Cul3A-3D in Fig. 2) using a 50 cm-long gauge auger (Cul2B, Cul2C and Cul3C) or a 70 cm-long and 4.5 cm wide PVC pipe (Cul2A, Cul3A, Cul3B and Cul3D). Cores collected with the gauge auger were sectioned in the field (every 2 cm in the top half and every 5 cm for the bottom half of the core) and samples were labelled and secured in plastic bags. PVC tubes were inserted in the soil until the top part was levelled with the surface, and then capped and removed with caution (see Fig. A.2a-c). The PVC core samples were frozen between sampling and analysis and were split lengthwise in the laboratory and sectioned using variable intervals, depending on the uniformity in sediment composition.

Individual slices from all cores were analysed for granulometry and organic matter (OM) content. The samples were oven-dried to remove water (at 60 °C for 3 days) and then treated with hydrogen peroxide (H_2O_2) to determine OM. Samples were weighed prior to and after each step, with the water and the OM content determined by the weight loss after oven-drying and hydrogen peroxide treatment, respectively. After OM destruction, the grain-size distribution of the coarse fraction ($\geq$63 μm) was determined by dry-sieving at 1/2-phi size intervals and of the fine fraction (<63 μm) using a laser particle size analyser. Grain-size distribution parameters (mean diameter, sorting, skewness and kurtosis) were calculated for all collected samples, using GRADISTAT v.8.0 (Blott and Pye, 2001). The compaction of the sediment in the PVC cores during penetration was corrected distributing the total shortening of the core to the sampled slices, assuming that the compaction ratio varies linearly with mud content. The same laboratory work process (water extraction, OM destruction, sieving and laser granulometry) was applied to the surface samples.

3.3. Vertical accretion rate assessment

The results of the core sample analysis in Culatra 2 and 3 were combined with the available raster datasets to estimate vertical accretion rates, by: a) identifying the depth within each core where the transition from a non-vegetated to a vegetated platform occurred and b) indirectly 'dating' this surface by inferring the potential year range since plant establishment from the available raster datasets. Given that the growth of salt marsh plants is linked to increased fine-grained sediment trapping (Pedersen and Bartholdy, 2007) and that both mineral and organic inputs are important for marsh vertical accretion (Neubauer, 2008; Rodriguez and McKee, 2021), the content in total fines (OM and mud, in %) was selected as a criterium that can account for both inputs. To identify the shift from a bare sandflat to a vegetated state, we assumed that a 'critical value' for total fines exists, below which the sediment can be considered as unvegetated sand with no significant organic and/or fine mineral deposition.

To reduce the uncertainty that can be associated with using a single threshold value, we opted for applying a range in threshold values, thus obtaining a range in vertical accretion since vegetation establishment. The threshold range used was determined by the total fines values identified in surface samples from vegetated and non-vegetated intertidal sites in the field (see section 4.1). The year of vegetation establishment was assessed as the period between the most recent flight in

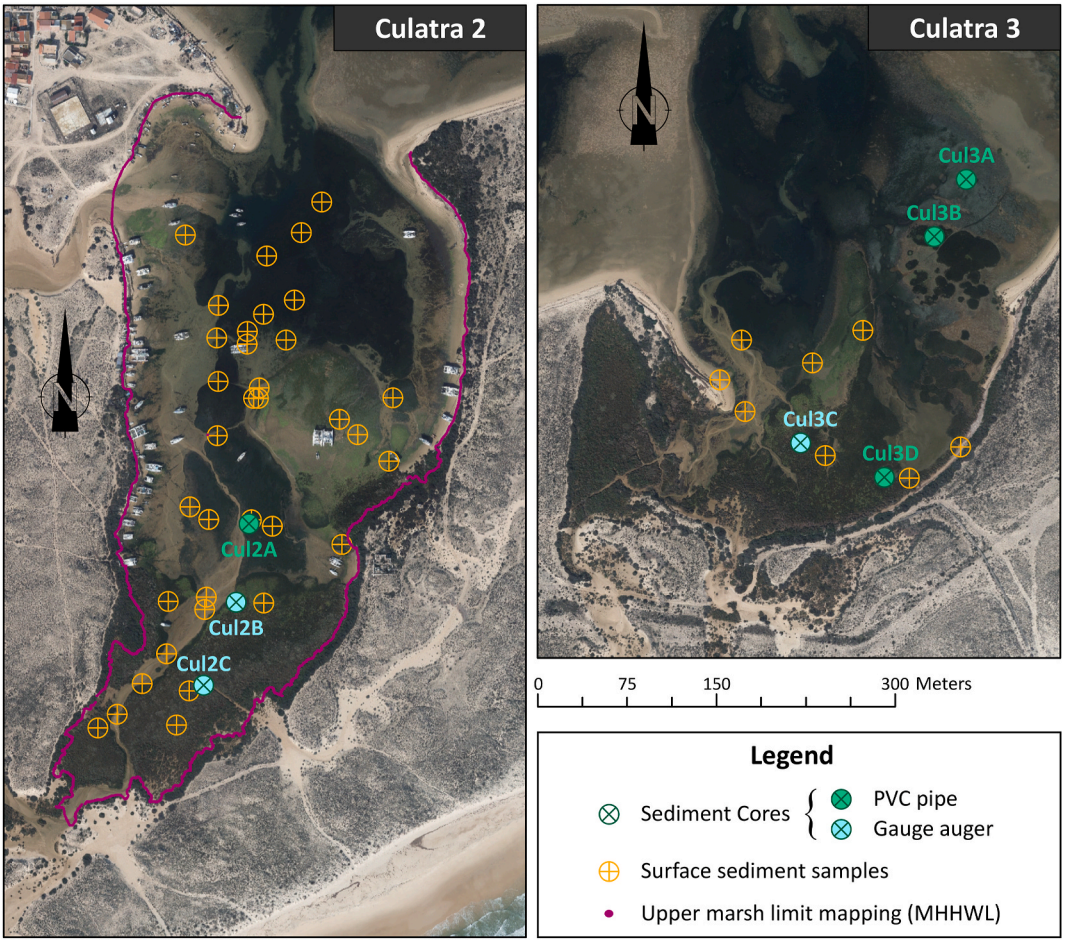

Fig. 2. Sediment surface sample and core (Cul2A to Cul2C and Cul3A to Cul3D) stations in Culatra 2 and Culatra 3. Topographic data for the mapped trajectory of the upper marsh limit (approximately at MHHW) is also shown (base: 2014 orthophotographs).

which the core station appeared unvegetated and the oldest flight in which vegetation was visible. This period, along with the core collection year, provided the maximum and minimum possible age for the vegetated intertidal habitat. From the range in vertical accretion height since plant establishment and the age range, a set of four vertical accretion rates was obtained, used to assess the average and standard deviation values in each location. The total, mineral and organic deposition rates (in gr/cm^2/yr) were also calculated by the sum of the weight of total, inorganic and organic deposition since marsh establishment (considering the average vertical accretion height), divided by the surface area of the core and the average age.

4. Results

4.1. Present-day distribution of plants and surface sediment properties

Two types of seagrasses, *Zostera noltei* (ZoN) and *Zostera marina* (ZoM), were identified in the field, the former present in both embayments (Culatra 2 and 3) and the latter present in the deeper, northern part near the entrance of Culatra 2 (Fig. 2). In terms of marsh plants, both embayments show a succession from *Spartina maritima* (SpM) in the low marsh, to *Salicornia ramosissima* (SaR) in the high marsh, and to *Limoniastrum monopetalum* (LiM) along the upper marsh border and the transition to the dune (Fig. A.3). Species, such as *Sarcocornia* perennis and *Limonium vulgare*, were also present in the high marsh, but with lower abundance. Surface sediment samples were grouped either by the dominant plant in each station, or in the bare sediment (BS) group. The results of the elevation and sediment analysis are given in Fig. 3 (spatially variable data for Culatra 2 are given in the Appendix, in Fig. A.1 and statistical metrics are given in Table A.1).

The plant zonation in the system is clearly depicted in the topographic data collected (Fig. 3a), with a transition from ZoM (sampled in Culatra 2) to ZoN (present in both bays) roughly at the low water neap tide level (MLWN). These elevational ranges are consistent with the different desiccation tolerance of the two seagrasses, restricting ZoM to the lower part of the intertidal zone (Leuschner et al., 1998), while ZoN typically exhibits exposure times of 6–8 h per semidiurnal tidal cycle (Silva and Santos, 2003). The transition from the tidal flat to the marsh (ZoN to SpM) takes place slightly above MSL (~0.1 m), while there is some mixing in species (SpM and SaR) at the transition between the two marsh zones (approximately at MHWN; Fig. 3a).

Bare sediment areas (BS in Fig. 3) show high variability in elevation, as samples were collected from various parts of the system. Both mud content and OM are low (median values of 1.6% and 0.9% respectively) and the samples comprise moderately to poorly sorted medium to coarse sands. The total fines content over bare sediment (sum of mud and OM for BS) ranges from 0.1 to 10.3%, with an average value of 3.4 ± 2.6% (see also Table A.1). This variability was the basis for setting the range in threshold values for total fines, used for identifying the shift from a non-vegetated sandy platform to a vegetated state in the cores, at 5–10% (in section 4.2.2).

Surface sediments collected from the ZoM meadow comprise very poorly sorted medium to coarse silt, with the lowest median diameter in the domain and the highest mud and OM (median values of 14.5 μm, 18.6% and 72%, respectively; Fig. 3). The areas occupied by ZoN show high variability in granulometry, ranging from coarse silt and very fine

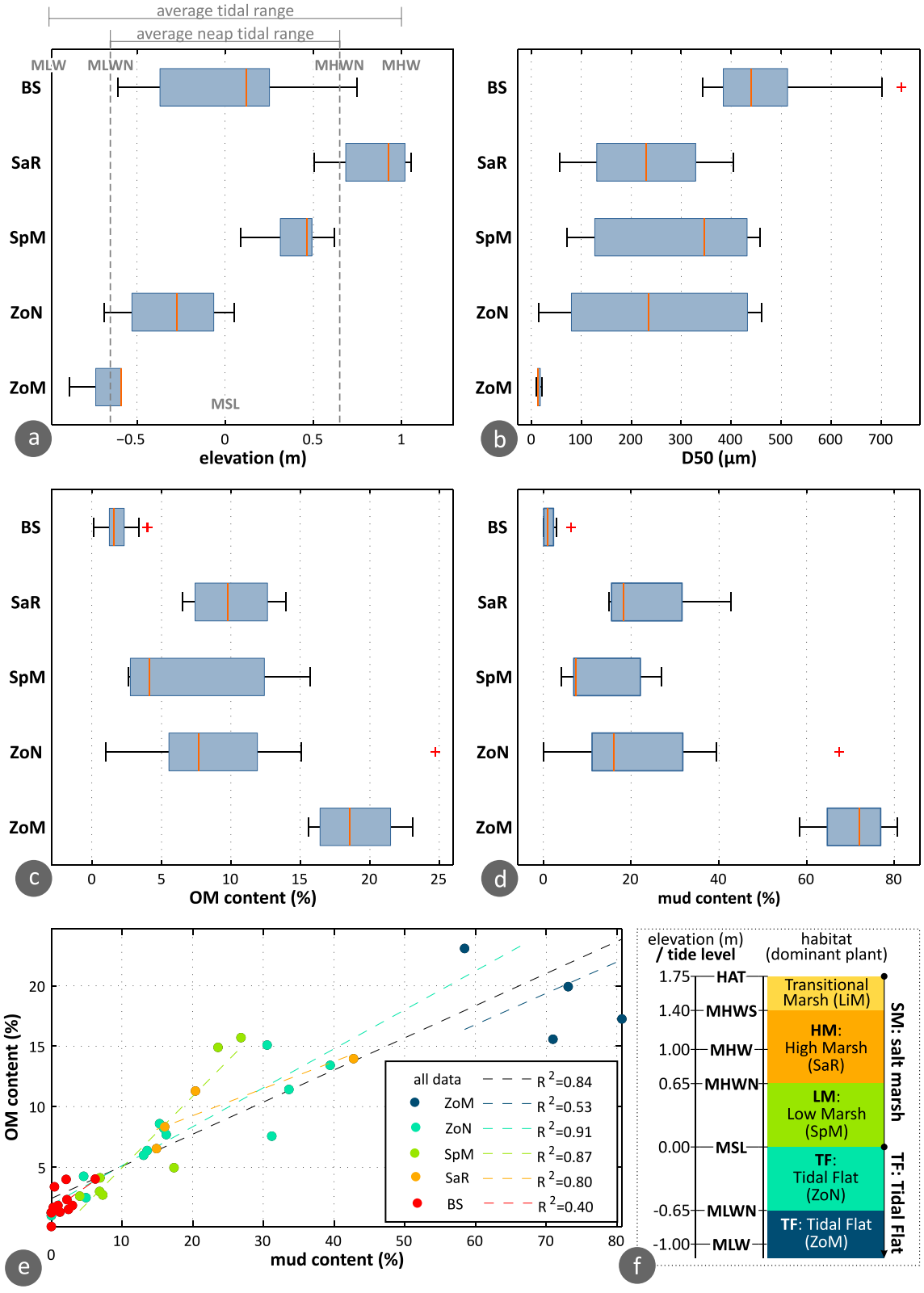

Fig. 3. Boxplots of topographic elevation (a; in m) and surface sediment sample results for median diameter (b; D50), organic matter (c; OM) and mud content (d) for non-vegetated areas (BS: bare sediment), and zones occupied with *Salicornia ramosissima* (SaR), *Spartina maritima* (SpM), *Zostera noltei* (ZoN) and *Zostera marina* (ZoM); median (orange line), 25th and 75th percentiles (blue box), minimum and maximum values (black lines) and outliers (red crosses) are shown. The correlation of mud and OM content in all samples, grouped by vegetation, is given in (e) and the relation between elevation, tidal level and intertidal habitats in the domain is summarised in (f) (LiM: *Limoniastrum monopetalum*).

Table 1
Accretion (average and standard deviation (StDev), in mm/yr) and deposition (total, organic and inorganic, in gr/cm^2/yr) rates since plant establishment, derived from the cores; z denotes elevation and corresponds to the time of core sampling.

Core	Habitat	z (cm)	Accretion rate (mm/yr)		Average deposition rate (gr/cm^2/yr)		
			Average	StDev	Total	Organic	Inorganic
Cul2A	TF	−22	3.0	1.8	0.15	0.01	0.14
Cul2B	LM	38	7.3	1.3	1.12	0.06	1.06
Cul2C	HM	92	1.3	0.3	0.23	0.03	0.21
Cul3A	TF	0	9.8	1.6	1.10	0.04	1.06
Cul3B	LM	23	4.5	2.5	0.55	0.01	0.54
Cul3C	LM	58	8.0	1.9	2.00	0.06	1.94
Cul3D	HM	63	5.5	1.2	0.68	0.04	0.64

sand in inner parts of seagrass patches, to coarse sands in locations close to the patch edge. The OM content is also variable and correlates strongly with the mud content (Fig. 3e; $R^2 = 0.91$). Over the low marsh (SpM), the surface sediment ranges from medium sands in regions bordering channels, to fine and very fine sands at elevations near the transition to the high marsh (D50 = 115–446 μm). Both mud and OM content distributions are right-skewed, showing high variability in values above the median (7.3% and 4.1%, respectively), with the two parameters positively correlated (Fig. 3e; $R^2 = 0.87$). Surface samples in the high marsh (SaR) show slightly finer sediment (230 μm) and higher OM (9.8%) than the SpM zones and, again, a positive linear relationship between mud and OM ($R^2 = 0.8$).

Sediment samples were collected at elevations of up to 1 m from MSL, meaning that the upper band of the high marsh was not sampled, collecting only topographic data within this zone. LiM, indicative of the rarely inundated areas of the domain (Contreras-Cruzado et al., 2017),

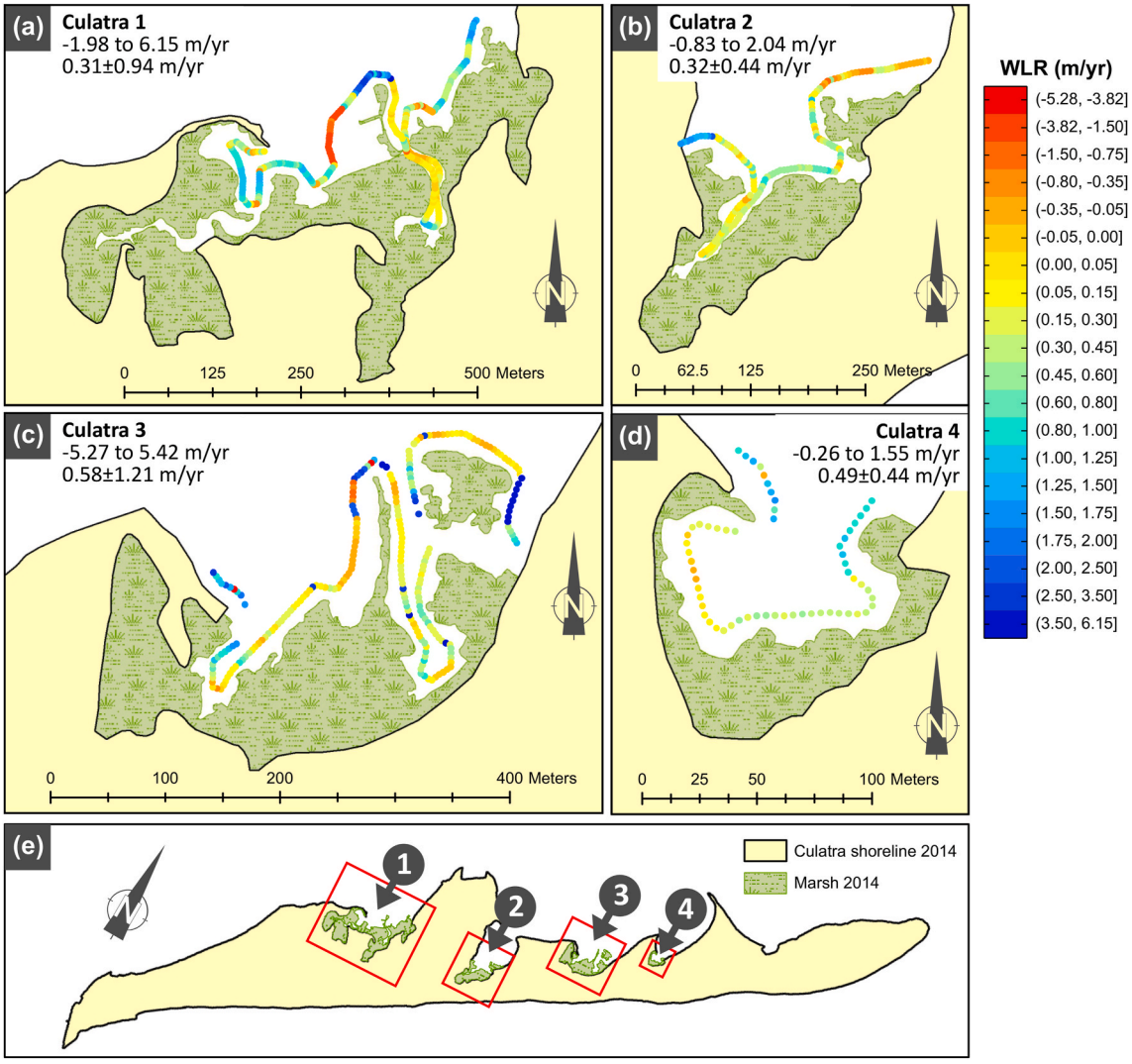

Fig. 4. Rates of marsh-edge boundary change in each embayment (Culatra 1 to 4: a to d, in m/yr, with reference to the colour-bar -blue to yellow colours denote progradation and orange to red colours denote retreat; value ranges and averages are noted in each plot), defined as WLR rates from all mapped marsh edge boundaries from the period 1952 to 2014; marsh polygons and the shoreline of 2014 are shown to assist interpretation. The boundaries of plots (a) to (d) on the island are shown in (e).

was used to identify the upper limit of the marsh in the field (transition from marsh to dune vegetation; see Fig. A.3); over non-vegetated areas the upper debris line was mapped, as indicator of MHHW level (mapped boundary shown in Fig. 2). The average elevation of the surveyed boundary was 1.5 ± 0.3 m, a value that is very close to the spring tidal amplitude in the system (Fig. 3f; MHWS to HAT: 1.4–1.75 m), verifying that LiM is a good indicator for the transitional marsh boundary. The average horizontal distance of the surveyed boundary and the back-barrier coastline mapped on the most recent orthophotograph (2014) was calculated at 1.6 ± 1.0 m. This relatively low error supports the accuracy of the visual criteria used to distinguish the upper boundary of the marsh in the raster dataset.

4.2. Long-term marsh morphological evolution

4.2.1. Horizontal rates and changes

The long-term (1952–2014) weighted linear regression (WLR) rates of the marsh edge boundary lines in Culatra 1 (Fig. 4a) are mostly positive (i.e., progradation), showing overall lateral growth. Negative rates (i.e., retreat) are mostly concentrated around the middle of the bay, coinciding with the shellfish farming zones in the area (Fig. 1b). Even though these activities take place within the lower intertidal zone, marsh horizontal expansion can be affected directly, through mechanical erosion (e.g., noted in Culatra 1 between 1996 and 2001), or indirectly, by restricting lateral marsh expansion. Rates in Culatra 2 (Fig. 4b) show overall progradation, with marsh edge retreat restricted in the eastmost marsh patch of the bay. Even through the impact of shorter-term stressors, like trampling by visitors and shellfish harvesters, cannot be assessed at the scale of our analysis, such activities have been linked to damage of saltmarsh vegetation and risks of wider scale erosion (Boorman, 2003; Goldman Martone and Wasson, 2008) and have potentially affected saltmarsh evolution in Culatra 2 (increased touristic and clam picking loads due to proximity to main settlement). Culatra 3 (Fig. 4c) shows high variability in terms of values and spatial distribution, along with the highest average rate among the embayments. Rates in Culatra 4 (Fig. 4d) are mostly positive, with higher progradation in the northern part of the bay and with retreat concentrated in the west inner part.

In terms of marsh total area, all embayments show similar evolution, with an initial phase of faster horizontal growth and a subsequent phase of reduced rates (Fig. 5a). The western, oldest marsh of the barrier (Culatra 1) grew rapidly ($1.37 \cdot 10^3$ m^2/yr) up to 1986 and with very low rates thereafter (around 100 m^2/yr). The same trend is observed in the second embayment (Culatra 2), with a rate of 791 m^2/yr up to 1986 and of 76 m^2/yr thereon. The marsh in Culatra 3 was expanding by an average of 1004 m^2/yr between 1980 and 2008 and maintained a near-stable area between 2008 and 2014. Culatra 4, the smallest and 'youngest' perched marsh of the island, showed rates of 346 m^2/yr up to 1986 and of 39 m^2/yr from then on.

To allow direct comparison between embayments, marsh areas were nondimensionalised with the available lateral accommodation space in each embayment, estimated by the 2011 DTM as the area lagoonwards from the backbarrier coastline with elevations exceeding 0.1 m above MSL (lowest elevation of marsh plants in the field; Fig. 3a). A uniform

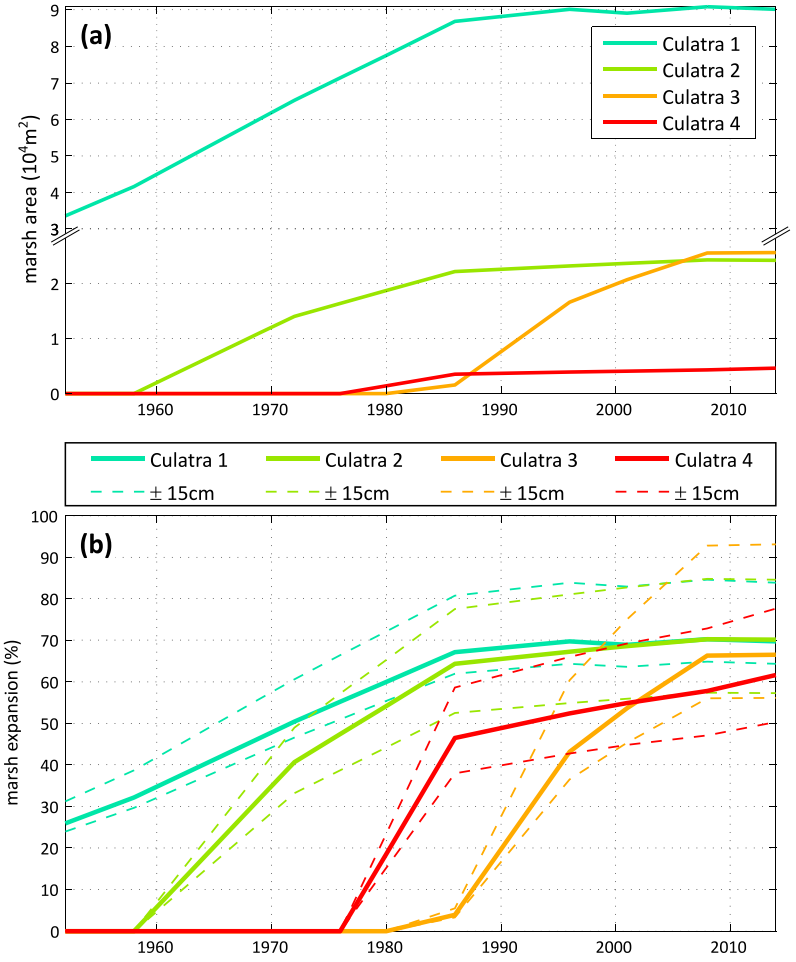

Fig. 5. Backbarrier marsh area evolution (a, in 10^4 m^2; note the break in the y axis) and percent march expansion (b, in %) for each of the four embayments (Culatra 1 to 4) with time; marsh expansion was calculated assuming stable available lateral accommodation space (2011 DTM) and dashed lines correspond to the vertical error of the DTM (±15 cm).

value for the available lateral accommodation space was applied for the entire period, in lack of past elevation data. This simplified approximation is solely intended to improve comparability of marsh growth between bay and not as an estimate of the actual marsh expansion timeseries, as it disregards eco-morphodynamic marsh evolution. The derived percentages are given in Fig. 5b (dashed lines account for the vertical error of the DTM; 0.15 m). Toward the end of the study period marsh expansion appears stabilised at values of 60–70% in all embayments. During the initial growth phase, the rates are rather similar for the younger perched marshes, with 2.3, 2.9 and 4.6 %/yr per year for Culatra 2, 3 and 4 (for 1958-86, 1986–2008 and 1976-86), respectively. Thereafter, growth slows down significantly in all embayments. The low rate of Culatra 1 until 1986 (1.2 %/yr) is attributed to the more mature state of the marsh, after which growth practically ceased.

4.2.2. *Vertical accretion rates*

The cores collected from Culatra 2 and 3 show that sediment tends to be finer and with higher OM and water content near the surface (Fig. 6), while there is high variability in sediment distribution between cores of similar elevation and habitat type. Coarser sediment (gravel) found in

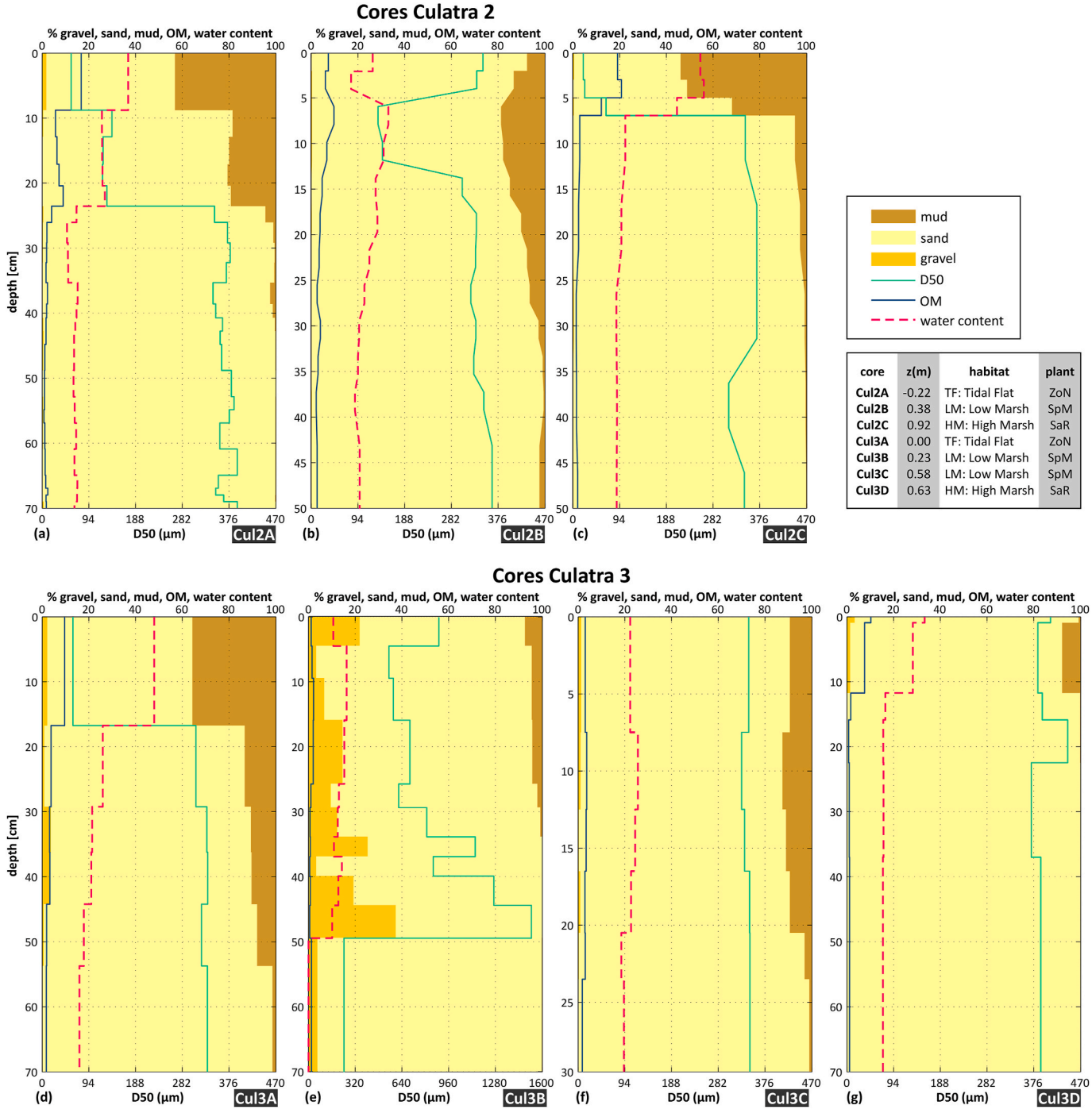

Fig. 6. Core granulometric composition as percentage of mud, sand and gravel content (stacked filled areas with reference to the top x-axis), median diameter (D50 (µm); cyan line with reference to the bottom x-axis, uniformly scaled, except for Cul3B), organic matter (OM) and water content (in %; solid blue and orange dashed lines, with reference to the top x-axis); a to c: cores collected from Culatra 2 (Cul2A-C); d to h: cores collected from Culatra 3 (Cul3A-D) (elevation (z), habitat and dominant plants are mentioned in the legend).

the surface layers of the cores are due to the presence of shell fragments, aside from Cul3B, where the origin is mostly lithogenic. Overall, the OM content is positively correlated to both mud and water content.

In Culatra 2, the core collected from the vegetated tidal flat (Cul2A; Fig. 6a) shows a surface layer (1–9 cm) of very coarse silt with high OM and water content, an intermediate layer (9–24 cm) of very fine to fine sands, with lower OM and water content, and a significantly coarser bottom layer (24–70 cm) comprising medium sands. The core from the low marsh (Cul2B; Fig. 6b) is more coarse-grained, comprising mainly fine (6–12 cm) to medium sands (0–4 cm and 14–50 cm). Considering the proximity of the core location to the border of the marsh platform (see Fig. 2), the coarser surface layer (0–4 cm) is likely due to a recent pulse in sand influx. The core collected from the high marsh (Cul2C; Fig. 6c) contains the finest sediment sampled in the bay, comprising a 4 cm surface layer of very poorly sorted coarse silt with high OM and water content, overlying moderately to moderately well sorted, very fine (5–7 cm) to medium sands (7–50 cm).

In Culatra 3, the core collected from the vegetated tidal flat (Cul3A; Fig. 6d) shows a wide surface layer (~44 cm) with high mud, OM and water content. The sediment in the upper 17 cm classifies as very coarse silt and the rest of the core as poorly to moderately well sorted medium sands. The low marsh core Cul3B (Fig. 6e) has a surprisingly high content of coarser sediment, that classifies as coarse to very coarse sands (D50 = 0.55–1.5 mm). The layers of increased gravel content likely correspond to pulses of increased marine sediment influx. Still, the presence of fines in the core is not negligible, with mud content exceeding 5% up to a depth of 16 cm. The low marsh core Cul3C (Fig. 6f) mainly comprises medium sands, with higher mud and water content within the topmost 20 cm and low OM throughout. It is noted that the sample collected from Cul3C extends to a depth of only 30 cm, due to disturbance of the sample within the bottom 20 cm during retraction of the gauge auger in the field. The core collected from the high marsh (Cul3D; Fig. 6g) consists of two rather uniform layers, a top one (0–12 cm) with higher mud, OM and water content and poorly to moderately sorted medium sands, and a base one (12–70 cm) comprising moderately well sorted medium sands, with low OM.

The coevolution between OM and fine sediment (i.e., mud content), identified in the surface sediment and in the core samples, supports the decision to include both parameters in the criterium used to separate the sedimentary facies pre- and post-vegetation establishment. The distribution of total fines along the core transects in the two bays is given in Fig. 7. The threshold values of 5% and 10% (yellow and white dashed lines, respectively) and the year range of vegetation (marsh plants or seagrasses) establishment, determined from the raster datasets (see Fig. A.4 and Fig. A.5 for Culatra 2 and 3, respectively), are marked for each core. Based on the threshold range applied, the height of sediment accumulated since plant establishment in Culatra 2 was assessed at 8–24 cm in Cul2A, 24–32.5 cm in Cul2B and 6–8 cm in Cul2C, while for Culatra 3 the values are 48–58 cm in Cul3A, 8.5–23 cm in Cul3B, 19–23 cm in Cul3C and 9–12 cm in Cul3D.

The derived age and height range for the layer deposited since the plant establishment, along with the sediment composition, were used to assess the vertical accretion and deposition rates since plant establishment, given in Table 1. The organic deposition rates are generally low, with the highest values recorded in the low marsh (Cul2B and Cul3C), indicating that mineral sedimentation produces the bulk of the accretion in all cores. The vertical accretion rates from cores from the same habitat were highly variable. The tidal flat core from Culatra 3 (Cul3A; 9.8 ± 1.6 mm/yr) showed 3 times faster accretion than the core from Culatra 2 (Cul2A; 3 ± 1.8 mm/yr). Similar and very high accretion rates were assessed over the low marsh in Cul2B and Cul3C (7.3 ± 1.3 and 8.1 ± 1.9 mm/yr), whereas in Cul3B the rate was half (4.5 ± 2.5 mm/yr). High marsh accretion rates show stark differences between the two bays, with core Cul2C (1.3 ± 0.3 mm/yr) barely having kept pace with SLR (1.5 ± 0.2 mm/yr; Dias and Taborda (1992)), whereas core Cul3D, located lower within the tidal frame, showed fast accretion (5.5 ± 1.2 mm/yr).

5. Discussion

5.1. Marsh vertical rates and sediment composition

Our results show higher vertical accretion in the low marsh (4.5–8 mm/yr) than in the high marsh (1.3–5.5 mm/yr), a trend that has been documented in other tidal marshes (i.e., Pethick (1981)). According to FitzGerald et al. (2008), low intertidal marsh plant species are more productive and contribute to higher rates of vertical accretion (~6–8

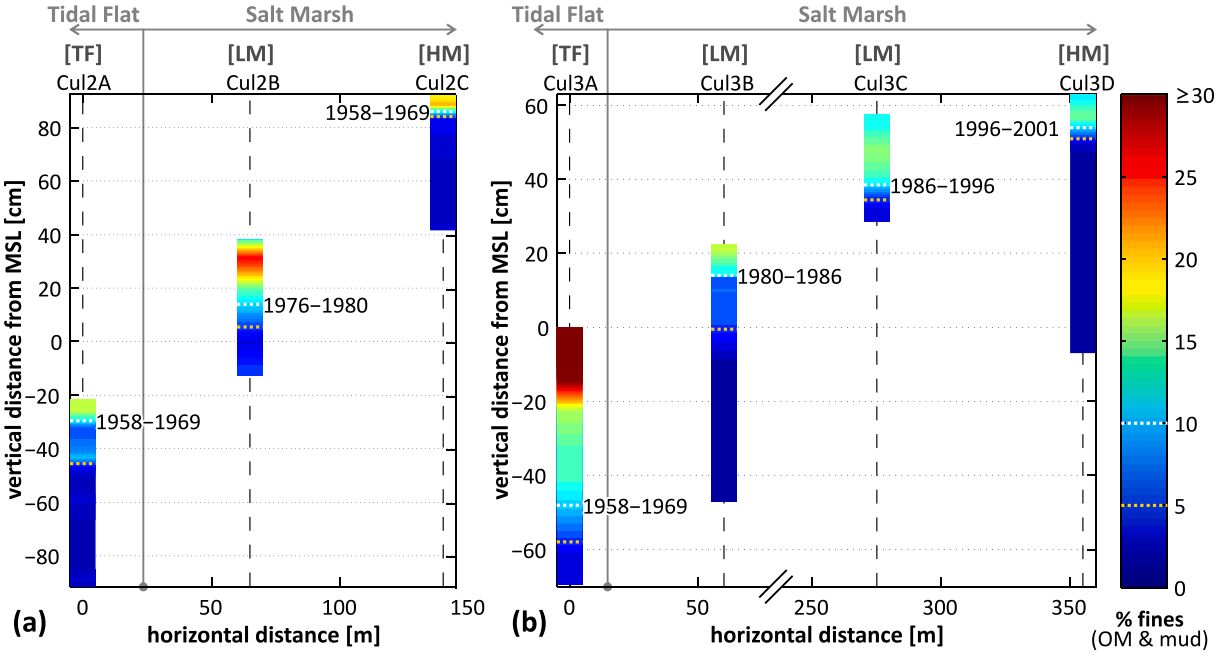

Fig. 7. Transects of total fines (mud and OM content; in %) in Culatra 2 and 3 (a and b; the vertical scale and the core width are exaggerated). Horizontal dashed lines on the cores denote the transition from bare sand flat to vegetated tidal flat/salt marsh (threshold value of 10% & 5% as white and yellow lines, respectively) and the plant establishment year range, assessed by the aerial photos, is noted next to each core.

mm/yr) than high marsh species (~2–3 mm/yr), with reduced inundation depths acting as a limiting factor on both tidal sedimentation and bioproductivity. This is also supported by the study of Kirwan et al. (2016), whose meta-analysis on data compiled from 179 unique measurements (USA, Canada, UK, France and Spain) suggests that, on average, low marshes accrete twice as fast as high marshes (mean rates of 6.9 mm/yr versus 3 mm/yr, respectively). Similar conclusions were drawn by accretion rates measured over low and high marsh sites in Narragansett Bay (USA), with high marshes tending to accrete at a rate close to the SLR due to their position within the tidal frame that limits flooding frequency (Bricker-Urso et al., 1989). Allen (2000) also affirms that the rate of vertical accretion in salt marshes is high at the first stage of their initiation and quickly slows down, as the marsh platform builds higher in the tidal frame.

The accretion rates of backbarrier marshes in Culatra are comparable to low marsh accretion rates from backbarrier and fringing patches in the western part of Ria Formosa and exceed estimates from neighbouring lagoon marsh patches. More specifically, long-term (1963–2000) rates over SpM in the backbarrier marsh of Ancão Peninsula (point CDSA1 in Fig. 1a) were estimated at 9.5 mm/yr (Arnaud-Fassetta et al., 2006), while short-term (over 1.5 years) accretion in a fringing marsh of the west part (point NC04 in Fig. 1a), also colonised by SpM, was assessed at 11.4 ± 2 mm/yr (Neumeier and Ciavola, 2004). Cores extracted from lagoon marsh patches near Faro-Olhão Inlet (points M22 in Fig. 1a) indicate rates of 1.5–3.8 mm/yr for the low marsh (SpM) and 1.6–4.3 mm/yr for the vegetated tidal flat (ZoN), with the lowest rates measured in the most exposed stations (Martins et al., 2022).

In terms of OM content variability along the intertidal habitats analysed, the core samples collected (top 5 cm) show high content over the tidal flat (ZoN; 10–17%), a reduction over the low marsh (SpM; 1.2–7.4%) and a subsequent increase in the high marsh (SaR; 8–20%); the same trend is reflected in the surface sediment samples (Fig. 3c; median values of 7.7, 4.1 and 9.8 for ZoN, SpM and SaR). Similar variability was reported by Contreras-Cruzado et al. (2017) along a transect in the mature backbarrier marsh of Tavira Island (point CC17 in Fig. 1a; 5 cm-height core samples), with the highest OM content in samples from the high marsh (>20%), followed by samples from low marsh habitats (13%). Studying the variability of OM stocks in the surface sediment in the lagoon intertidal habitats near the Faro-Olhão Inlet (points M22 in Fig. 1a), de los Santos et al. (2022) found that OM values decreased along the transition from the seagrass meadow (ZoN) to the low marsh (SpM) and that hydrodynamically exposed locations contained 1.5 times less OM than more protected areas. Hydrodynamic exposure could be related to the reduced OM content at the surface of the cores of Culatra 3, compared to Culatra 2 (by 1.6 times for ZoN and 2.5–6 times for SpM).

Overall, the contribution of organic deposition in the intertidal habitats of Culatra is very limited compared to the mineral part, suggesting that the accretionary process is still at a juvenile stage (Boyd and Sommerfield, 2016). The correlation of deposited organic matter since marsh establishment with accretion rate is significantly poorer than that of the inorganic stock (Fig. A.6; $p = 1.2{\cdot}10^{-3}$ and $p = 7.3{\cdot}10^{-5}$, respectively), indicating that abiotic factors are the main driver for marsh accretion and there is high disparity in the influence of biotic factors. The high influence of local factors is also supported by the variability in vertical rates identified. This influence may become less pronounced with time and distance from the marsh edge, as the marsh builds higher within the tidal frame (Allen, 2000; Stoddart et al., 1989). Still, the low organic deposition of the recently formed backbarrier marshes of Culatra poses questions on the accuracy and validity of largescale assessments of blue carbon storage potential based on plant mappings (e.g., from remotely sensed data).

Young backbarrier marshes, like the ones in Culatra 2 and 3, would be expected to grow faster than older ones, as accretion rates generally reduce exponentially with time (Allen, 2000; De Groot et al., 2011). There is evidence however that contradicts this commonly accepted paradigm of decreasing sedimentation rates with increasing age of the marsh (Schuerch et al., 2018). A comparison of vertical growth rates since marsh establishment of Culatra with other recently (within the last century) established and similar in terms of dynamics backbarrier marshes (see Fig. A.7 for details on key drivers across relevant spatial scales in each site; methodology after Yando et al. (2023)) are given in Table 2. The accretion balance rates (accretion rate minus synchronous regional SLR; (Crosby et al., 2016)) from Culatra are toward the higher end of the range. The low marsh accretion balance rate at the Skallingen spit (Danish Wadden Sea; Nielsen and Nielsen (2002)) is comparable to the similarly young low marshes of Culatra. Over the high marsh sites of Skallingen, however, older marsh sites show higher vertical rates, indicating the influence of local conditions (e.g., sediment import through ice-rafting) and morphology (e.g., location of creeks) to vertical accretion. The low accretion balance throughout the backbarrier marsh transect in the barrier of Sylt (German Wadden Sea; Schuerch et al. (2012))indicates the importance of oceanic forcing (e.g., storm frequency and intensity, SLR) to backbarrier dynamics. Similarly, sediment delivery (e.g., distance to creek and marsh edge) appears more important in controlling marsh accretion balance than age in young (non-subsiding) backbarrier marshes of the Dutch Wadden Sea (Terschelling and Schiermonnikoog; van Dobben et al. (2022)). Despite being older, the accumulation balance since low marsh establishment in the Ancão Peninsula of Ria Formosa (core CDSA1 in Table 2) exceeds the rates of Culatra. This enhanced accretion is due to the presence of washover and aeolian sand layers within the core posterior to the initial marsh establishment (Arnaud-Fassetta et al., 2006), indicating the importance of sand mineral deposition. These differences draw attention to the critical role that local factors may play during the early-stage marsh evolution. The success of projects using nature-based solutions, like the backbarrier saltmarsh construction to enhance future barrier resilience in Cedar Island (Virginia barrier chain, USA; Hein et al. (2021)), will depend heavily on the response of the implemented design to local conditions.

5.2. Mechanisms of backbarrier marsh genesis and early-stage evolution

Information on the geomorphological changes and major processes that led to the formation of the initial sandy platform prior to the establishment of marsh vegetation can be drawn from the available raster datasets. The earliest available aerial photograph of 1947 (Fig. A.8a) shows that the present-day marsh platform at the southern part of Culatra 2 (e.g., Cul2C) appears to be on top of washover deposits. This event was likely associated to the cyclone of 1941, during which severe damage was reported in the island settlement (Garnier et al., 2018). From the same aerial photo, it appears that elevations prior to plant establishment were already increasing from the tidal flat to the high marsh core (Cul2A to Cul2C). Culatra 3 was captured for the first time in the flight of 1958 (Fig. A.8b) and a large part of the current topography in Culatra 3 is the result of inlet morphodynamic processes (recurved spit formation and incorporation of flood shoals). Even though the phase when the eastern tip of Culatra was at the location of the cores (sometime between 1952 and 1958) is not captured in aerial photos, the inherited recurved spit deposits in the barrier directly seawards from the bay are still visible in the current topography (Fig. 1b & Fig. A.8c). In the 1958 aerial photo, the two highest cores (Cul3C and Cul3D) appear to be atop a spit end, the intermediate core (Cul3B) is at the edge of a posterior, presumably lower, spit end and the tidal flat core (Cul3A) is located at the edge of delta shoal deposits. It is important to note that, based on the location of the debris line in the rasters (1947 for Culatra 2 and 1958 for Culatra 3), and on the fact that the deposits at the location of the cores were subaerial during image capture, it can be deduced that the surface of the deposited sand was within the intertidal zone in all core locations. The elevation of the sandy platform within the cores (Fig. 7) also indicates that the sandy substrate created by these processes was adequate for plant (marsh plant/seagrass) colonisation.

Table 2
Synthesis of backbarrier marsh age and vertical accretion rates since marsh establishment (fines layer thickness divided by average marsh age), Regional SLR (RSLR) rates and derived accretion balance rate (accretion minus RSLR rate; Crosby et al. (2016)) from the Frisian Islands and Ria Formosa (LM: Low Marsh, HM: High Marsh). RSLR rates (contemporaneous with accretion period, or uniform long-term values when reliable shorter-term estimates were unavailable) were obtained from the same publication, apart from the Dutch Wadden Sea (data from Keizer et al. (2023)) and Ria Formosa (data from Dias and Taborda (1992)).

Barrier | Location (Reference)						
core station	marsh age (yr)	fines layer thickness (mm)	RSLR (mm/yr)	accretion rate (mm/yr)	accretion balance (mm/yr)	marsh habitat
Skallingen | Danish Wadden Sea (Nielsen and Nielsen, 2002)						
inner marsh	58	165	1.3	2.8	1.6	HM
inner wadden	48	100	1.2	2.1	0.9	HM
outer marsh (west)	58	160	1.3	2.8	1.5	HM
outer marsh (east)	98	290	1.1	3.0	1.9	HM
outer marsh (east)	25	170	3.8	6.8	3.0	LM
Sylt | German Wadden Sea (Schuerch et al., 2012)						
S1	68–88	85	2.1	1.1	−1.0	HM
S2	88–98	270	2.1	2.9	0.8	LM
S3	13–20	45	2.1	2.7	0.6	LM
Terschelling | Dutch Wadden Sea (van Dobben et al., 2022)						
TER_T3	64–77	150	2.1	2.1	0.0	HM
TER_T4	77–90	247	2.0	3.0	0.9	LM
Schiermonnikoog | Dutch Wadden Sea (van Dobben et al., 2022)						
SCH_T5	89–98	140	2.0	1.5	−0.5	LM
SCH_T3	32–47	97	2.3	2.5	0.2	LM
SCH_T2	22–37	135	2.5	4.6	2.1	LM
SCH_T1	22–37	65	2.5	2.2	−0.3	LM
SCH_T0	3–25	41	2.7	2.9	0.2	LM
Ancão | Ria Formosa, Portugal (Arnaud-Fassetta et al., 2006)						
CDSA1	84–94	800*	1.5	9.0	7.5	LM
** sands present: from 1 major washover (~10 cm) and 4 minor washover or aeolian deposits*						
Culatra | Ria Formosa, Portugal (this study)						
Cul2B	37–41	283	1.5	7.3	5.8	LM
Cul2C	48–59	70	1.5	1.3	−0.2	HM
Cul3B	32–38	158	1.5	4.5	3.0	LM
Cul3C	22–32	210	1.5	8.0	6.5	LM
Cul3D	17–22	105	1.5	5.5	4.0	HM

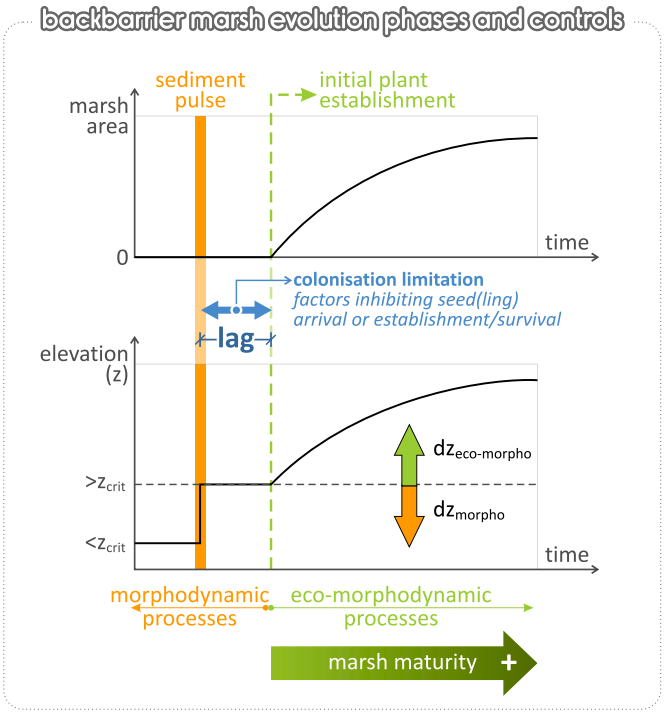

Fig. 8. Summary of main phases and controls on backbarrier marsh evolution, derived from the data collected in Culatra (the graphic representation is inspired by the response of estuarine marshes to sediment pulses, shown in Mudd (2011)); z_{crit} is the elevation limit for the development of marsh vegetation (approximately at MWL) and $z_{morpho}/z_{eco\text{-}morpho}$ denotes the shift in elevation from morphodynamic to eco-morphodynamic processes.

Culatra 4 was also impacted by overwash, with aerial photos from 1969 (and 1972 see Fig. A.8c) showing a washover fan over the southern part of the bay, where marshes subsequently developed. The event was likely associated with the 1961 and/or the 1969 storms that hit the area (Garcia et al., 2010). After the mid-1970s, overwash frequency in east Culatra reduced significantly (Garcia et al., 2010), indicating the gradual establishment of more stable backbarrier conditions.

It follows that the present-day backbarrier marsh platforms in the three eastern bays of Culatra have been largely inherited by sediment deposits, introduced to the backbarrier environment during the rapid elongation phase of the island, either by incorporation of recurved spit and flood deltas (Pilkey et al., 1989), or during overwash of the newly formed low-lying barrier (Garcia et al., 2002; Matias et al., 2008). Information on bay formation and introduction of intertidal deposits within Culatra 2, 3 and 4 is compiled in Table 3.

Following the introduction of backbarrier deposits and the formation of the sandy platform, a delay in the establishment of marsh vegetation was noted in all three bays, which is estimated by the photos at 22.5 ± 7.8, 33 ± 11.3 and 13 ± 8.5 years for Culatra 2, 3 and 4 (Table 3). Such delays have been observed in other systems, such as salt marsh restoration attempts in the Tijuana Estuary (California, USA), where limited seed dispersal was observed even 5 years after the reestablishment of tidal flushing (Morzaria-Luna and Zedler, 2007) and in the Blackwater Estuary (UK), where plant establishment delayed 7 years (Wolters et al., 2005). A significantly longer lag of 200 years between sand platform formation and marsh establishment, noted in the Skallingen spit backbarrier, was attributed to a lack of fine sediment deposition and/or symbiotic fungi vital for plant colonisation (Bartholdy et al., 2018).

Generally, a lag in marsh plant establishment occurs when colonisation is restricted by factors such as: a) connectivity and distance to the main seed sources, leading to insufficient seed arrival, and b) environmental factors (i.e., inundation regime, currents) inhibiting seedling emergence and survival (Lõhmus et al., 2020). Due to the proximity of

Table 3
Synopsis of the characteristics and main events during the pre- and post-establishment of backbarrier vegetation (morphodynamic and eco-morphodynamic periods, respectively) in each bay.

Dominant processes	Event	Type	Embayment		
			Culatra 2	Culatra 3	Culatra 4
Morpho-dynamic	Embayment	Formation[a]	1930–1941	1952–1958	1958–1969
		Opening (m)	100	250	60
		Area (m^2)	120,000	30,400	10,000
		Indentation[b]	very high	low	medium-high
	Sediment pulse	Year	1941	1952–1958	1961 and/or 1969
		Mechanism	storm overwash	inlet delta shoals	storm overwash
Eco-morpho-dynamic	Marsh plant establishment	Year	1958–1969	1980–1996[c]	1976–1980
		Lag (yr)	22.5 ± 7.8	33.0 ± 11.3	13.0 ± 8.5

[a] *Start of bay formation period*: Last flight where the bay was inexistent. *End of bay formation period*: Storm (or most recent storm) responsible for the overwash sediment pulse in the backbarrier (Culatra 2 & 4) or first flight where the bay is documented for sediment pulse due to inlet delta shoals (Culatra 3; in this case, the bay formation and the sediment pulse periods are the same).
[b] Classification after Bowman et al. (2014); related indentation indexes given in section 2.1.
[c] 1986 is excluded due to the low expansion (Fig. 5a).

the embayments to lagoon marshes (Fig. 1a) and to pre-existing backbarrier marshes (in Culatra 1 and in nearby Armona Island), seed availability should not have been restricted in the area. On the other hand, the limiting influence of the inundation regime, if any, should largely be similar between embayments and cannot justify the decade-scale difference in lag between them (Table 3). Therefore, hydrodynamics appears to be the only major controlling factor that could explain these differences in lag between bays. The covariation between lag and embayment opening (Table 3) leads us to assume that morphological differences promoted different hydrodynamic conditions within the bays. The wide opening of Culatra 3 indicates high exposure to hydrodynamics and therefore a stronger dependency on the tidal currents along the backbarrier. This suggests that favourable hydrodynamic conditions within Culatra 3 appeared only after the tidal prism balance of the neighbouring Armona Inlet had sufficiently reduced, causing a longer delay for plant establishment in the bay. Contrastingly, the narrow opening of Culatra 4 readily provided a lower-energy environment, allowing for earlier establishment of marsh plants. A similar lag (11 years) was observed at a narrow-opening embayment in the backbarrier of Cabanas Island (point K20 in Fig. 1a; Kombiadou et al. (2020)). Considering the low distance of this site to mainland and the low tidal flow along the backbarrier (evidenced by frequent dredging of the channel; Dias et al. (2003)), it appears that a lag of roughly a decade might be typical for backbarrier marsh establishment under low energy conditions within the Ria Formosa system. A decadal timescale is also reported for natural patch marsh formation in other backbarrier systems (e.g., Bogue Banks, USA; Rodriguez and McKee (2021)). The 20-year lag of Culatra 2 falls in-between the two, pointing to intermediate conditions. Based on the work of De Groot et al. (2011), the gradual transition from sandy to finer sediment in the cores of Culatra 2 and 3 (transition from sandy substrate to marsh Fig. 6), also points to energetic conditions during initial marsh formation in the two bays.

Based on the analysis performed, three main phases can be identified during early backbarrier marsh establishment, summarised in Fig. 8. The initial phase, dominated by morphodynamic processes, is preconditioned by the need to build the sandy substrate sufficiently high within the intertidal zone to allow for marsh plant establishment ($>z_{crit}$, approximately at MWL). In backbarrier settings, this is often achieved by a sediment pulse from overwash or delta shoal incorporation. After the formation of an adequately elevated sandy platform, a lag for plant establishment is observed, with durations that can vary significantly, depending on local conditions: a decade-scale lag can be expected in areas of low energy (e.g., protected bays) and low distance from seed sources, while a multidecadal lag can occur in highly exposed areas (e.g., open bays). It would be logical to assume that these lags would be longer under conditions of low seed availability. After initial establishment, eco-geomorphodynamic processes begin to control vertical growth ($dz_{eco\text{-}geomorpho}$) and lateral expansion, initially progressing rapidly and gradually slowing down, as plants expand and occupy the available accommodation space (Fig. 8).

6. Concluding remarks

The main conclusions drawn from the analysis are summarised as follows:

- The disparity in accretion balance rates between values assessed for Culatra and values from similarly young backbarrier marshes (Frisian Islands) highlights the importance of local conditions (sediment import, distance to creeks and marsh edge, storm frequency and intensity) to marsh build-up, even during the early stage after plant establishment. The wide range in accretion rates assessed for the same intertidal vegetated habitat (high marsh: 1.3–5.5 mm/yr, low marsh: 4.5–8.1 mm/yr, vegetated tidal flat: 3–9.8 mm/yr) indicates high spatial variability in the major drivers of growth, such as hydrodynamics and mineral sediment delivery, in the domain, even within the same backbarrier system and within the same embayment.
- In backbarrier embayments with low fine sediment influx, like Culatra, the presence of marine sands is prevalent, even after the establishment of intertidal plants. The sediment is predominantly sandy, with low organic deposition, even near the marsh surface, indicating the dominance of mineral deposition to vertical accretion, especially for juvenile backbarrier marshes.
- Recent backbarrier marsh genesis in Culatra was initiated by the introduction of intertidal deposits (through overwash or inlet shoals) that provided a sandy platform, suitable for marsh plant establishment. A lag of ca. 10–30 years was observed until colonisation was established, mainly driven by local hydrodynamic conditions. The lower end of the range was observed in protected embayments, which could indicate that it reflects a 'typical' lag for backbarriers in the system, while the upper end of the range was linked to higher energy embayments.
- After plant establishment, backbarrier marsh horizontal growth at the macroscale of a bay appears conditioned by the form of the initial intertidal deposit, with reducing rates with time, as plants expand and occupy the available accommodation space. At a more detailed spatial scale, long-term horizontal rates of the lagoonside marsh edge are highly complex, with areas of chronic retreat likely related to human pressures (i.e., shellfish farming in Culatra 1 and boat mooring in Culatra 2) or to hydrodynamics (i.e., central part of Culatra 3).

CRediT authorship contribution statement

Katerina Kombiadou: Writing – review & editing, Writing – original draft, Visualization, Validation, Methodology, Investigation, Formal analysis, Data curation, Conceptualization. **A. Rita Carrasco:** Writing – review & editing, Validation, Methodology, Investigation, Conceptualization. **Susana Costas:** Writing – review & editing, Validation, Methodology, Investigation, Conceptualization. **Margarida Ramires:** Methodology, Formal analysis, Data curation. **Ana Matias:** Writing – review & editing, Validation, Supervision, Project administration, Methodology, Investigation, Funding acquisition, Conceptualization.

Declaration of competing interest

The authors declare that they have no known competing financial interests or personal relationships that could have appeared to influence the work reported in this paper.

Data availability

Data will be made available on request.

Acknowledgements

The fieldwork, laboratory analysis and coastline mapping were conducted in the framework of the EVREST project, funded the Fundação para a Ciência e a Tecnologia (FCT), Portugal, through grant number PTDC/MAREST/1031/2014. During elaboration of the manuscript, K. Kombiadou was supported by the contract CEECINST/00146/2018/CP1493/CT0011, A.R. Carrasco by the contract CEECINST/00052/2021/CP2792/CT0007 and S. Costas by the contract 2021.04286. CEECIND, all funded by FCT. The authors also recognise the support of national funds through FCT, under the project LA/P/0069/2020, granted to the Associate Laboratory ARNET, and project UID/00350/2020, granted to CIMA.

We would also like to thank Luisa bon de Sousa, Emily Robbins, Marine Fouin and Victoria Celedón for their participation and assistance during fieldwork campaigns and Mónica Martins for her assistance with halophytic plant identification.

Appendix A. Supplementary data

Supplementary data to this article can be found online at https://doi.org/10.1016/j.ecss.2023.108589.

References

Allen, J.R.L., 2000. Morphodynamics of holocene salt marshes: a review sketch from the Atlantic and southern North sea coasts of Europe. Quat. Sci. Rev. https://doi.org/10.1016/S0277-3791(99)00034-7.

Andrade, C., Freitas, M.C., Moreno, J., Craveiro, S.C., 2004. Stratigraphical evidence of Late Holocene barrier breaching and extreme storms in lagoonal sediments of Ria Formosa, Algarve, Portugal. Mar. Geol. 210, 339–362. https://doi.org/10.1016/J.MARGEO.2004.05.016.

Antunes, C., 2019. Assessment of sea level rise at West Coast of Portugal Mainland and its projection for the 21st century. J. Mar. Sci. Eng. 7, 61. https://doi.org/10.3390/jmse7030061.

Antunes, C., Taborda, R., 2009. Sea level at Cascais tide gauge: data, analysis and results. J. Coast. Res. SI 56, 218–222.

Arnaud-Fassetta, G., Bertrand, F., Costa, S., Davidson, R., 2006. The western lagoon marshes of the Ria Formosa (Southern Portugal): sediment-vegetation dynamics, long-term to short-term changes and perspective. Continent. Shelf Res. 26, 363–384. https://doi.org/10.1016/j.csr.2005.12.008.

Bartholdy, J., Brivio, L., Bartholdy, A., Kim, D., Fruergaard, M., 2018. The Skallingen spit, Denmark: birth of a back-barrier saltmarsh. Geo Mar. Lett. 38, 153–166. https://doi.org/10.1007/s00367-017-0523-5.

Belliard, J.P., Temmerman, S., Toffolon, M., 2017. Ecogeomorphic relations between marsh surface elevation and vegetation properties in a temperate multi-species salt marsh. Earth Surf. Process. Landforms 42, 855–865. https://doi.org/10.1002/esp.4041.

Blott, S.J., Pye, K., 2001. GRADISTAT: a grain size distribution and statistics package for the analysis of unconsolidated sediments. Earth Surf. Process. Landforms 26, 1237–1248. https://doi.org/10.1002/esp.261.

Boorman, L., 2003. Saltmarsh Review: an Overview of Coastal Saltmarshes, Their Dynamic and Sensitivity Characteristics for Conservation and Management (JNCC Report No. 334). Peterborough.

Bowman, D., Rosas, V., Pranzini, E., 2014. Pocket beaches of Elba Island (Italy) – planview geometry, depth of closure and sediment dispersal. Estuar. Coast Shelf Sci. 138, 37–46. https://doi.org/10.1016/j.ecss.2013.12.005.

Boyd, B.M., Sommerfield, C.K., 2016. Marsh accretion and sediment accumulation in a managed tidal wetland complex of Delaware Bay. Ecol. Eng. 92, 37–46. https://doi.org/10.1016/j.ecoleng.2016.03.045.

Bricker-Urso, S., Nixon, S.W., Cochran, J.K., Hirschberg, D.J., Hunt, C., 1989. Accretion rates and sediment accumulation in Rhode Island salt marshes. Estuaries 12, 300–317. https://doi.org/10.2307/1351908.

Cabaço, S., Alexandre, A., Santos, R., 2005. Population-level effects of clam harvesting on the seagrass Zostera noltii. Mar. Ecol. Prog. Ser. 298, 123–129. https://doi.org/10.3354/meps298123.

Cabral, S., Alves, A.S., Castro, N., Chainho, P., Sá, E., Cancela da Fonseca, L., Fidalgo e Costa, P., Castro, J., Canning-Clode, J., Pombo, A., Costa, J.L., 2019. Polychaete annelids as live bait in Portugal: harvesting activity in brackish water systems. Ocean Coast Manag. 181, 104890 https://doi.org/10.1016/j.ocecoaman.2019.104890.

Carrasco, A.R., Ferreira, Ó., Davidson, M., Matias, A., Dias, J.A., 2008. An evolutionary categorisation model for backbarrier environments. Mar. Geol. 251, 156–166. https://doi.org/10.1016/j.margeo.2008.02.009.

Carrasco, A.R., Kombiadou, K., Amado, M., Matias, A., 2021. Past and future marsh adaptation: lessons learned from the Ria Formosa lagoon. Sci. Total Environ. 790, 148082 https://doi.org/10.1016/j.scitotenv.2021.148082.

Carrasco, A.R., Plomaritis, T., Reyns, J., Ferreira, Ó., Roelvink, D., 2018. Tide circulation patterns in a coastal lagoon under sea-level rise. Ocean Dynam. https://doi.org/10.1007/s10236-018-1178-0.

Contreras-Cruzado, I., Infante-Izquierdo, M.D., Márquez-García, B., Hermoso-López, V., Polo, A., Nieva, F.J.J., Cartes-Barroso, J.B., Castillo, J.M., Muñoz-Rodríguez, A., 2017. Relationships between spatio-temporal changes in the sedimentary environment and halophytes zonation in salt marshes. Geoderma 305, 173–187. https://doi.org/10.1016/j.geoderma.2017.05.037.

Costas, S., Ramires, M., de Sousa, L.B., Mendes, I., Ferreira, O., 2018. Surficial sediment texture database for the south-western Iberian Atlantic margin. Earth Syst. Sci. Data 10, 1185–1195. https://doi.org/10.5194/essd-10-1185-2018.

Crosby, S.C., Sax, D.F., Palmer, M.E., Booth, H.S., Deegan, L.A., Bertness, M.D., Leslie, H. M., 2016. Salt marsh persistence is threatened by predicted sea-level rise. https://doi.org/10.1016/j.ecss.2016.08.018.

De Groot, A.V., Veeneklaas, R.M., Bakker, J.P., 2011. Sand in the salt marsh: contribution of high-energy conditions to salt-marsh accretion. Mar. Geol. 282, 240–254. https://doi.org/10.1016/J.MARGEO.2011.03.002.

de los Santos, C.B., Lahuna, F., Silva, A., Freitas, C., Martins, M., Carrasco, A.R., Santos, R., 2022. Vertical intertidal variation of organic matter stocks and patterns of sediment deposition in a mesotidal coastal wetland. Estuar. Coast Shelf Sci. 272 https://doi.org/10.1016/J.ECSS.2022.107896.

Dias, J.A., Ferreira, Ó., Matias, A., Vila-Concejo, A., Sá-Pires, C., 2003. Evaluation of soft protection techniques in barrier islands by monitoring programs: case studies from Ria Formosa (Algarve-Portugal). J. Coast Res. https://doi.org/10.2307/40928755.

Dias, J.A., Taborda, R., 1992. Tidal gauge data in deducing secular trends of relative Sea Level and crustal movements in Portugal. J. Coast Res. 8, 655–659.

Esaguy, A.S., 1984. Ria de Faro. Barra da Armona. Evolução 1873-1983. Lisbon.

Fagherazzi, S., Mariotti, G., Leonardi, N., Canestrelli, A., Nardin, W., Kearney, W.S., 2020. Salt marsh dynamics in a period of accelerated Sea Level rise. J. Geophys. Res. Earth Surf. 125, e2019JF005200 https://doi.org/10.1029/2019JF005200.

FitzGerald, D.M., Fenster, M.S., Argow, B.A., Buynevich, I.V., 2008. Coastal impacts due to sea-level rise. Annu. Rev. Earth Planet Sci. 36, 601–647. https://doi.org/10.1146/ANNUREV.EARTH.35.031306.140139.

FitzGerald, D.M., Hughes, Z., 2019. Marsh processes and their response to climate change and sea-level rise. Annu. Rev. Earth Planet Sci. 47, 481–517. https://doi.org/10.1146/annurev-earth-082517-010255.

FitzGerald, D.M., Hughes, Z.J., 2021. State of salt marshes. In: Salt Marshes. Cambridge University Press, pp. 1–6. https://doi.org/10.1017/9781316888933.001.

French, J., 2019. Tidal salt marshes: sedimentology and geomorphology. In: Perillo, G.M. E., Wolanski, E., Cahoon, D.R., Hopkinson, C.S. (Eds.), Coastal Wetlands: an Integrated Ecosystem Approach. Elsevier, pp. 479–517. https://doi.org/10.1016/B978-0-444-63893-9.00014-9.

Garcia, T., Ferreira, Ó., Matias, A., Dias, J.A., 2010. Overwash vulnerability assessment based on long-term washover evolution. Nat. Hazards 54, 225–244. https://doi.org/10.1007/s11069-009-9463-3.

Garcia, T., Ferreira, Ó., Matias, A., Dias, J.A., 2002. Recent evolution of Culatra island (Algarve – Portugal). In: Gomes, F.V., Taveira Pinto, F., das Neves, L. (Eds.), Littoral 2002: 6th International Symposium Proceedings: A Multi-Disciplinary Symposium on Coastal Zone Research, Management and Planning, pp. 289–294. Porto.

Garnier, E., Ciavola, P., Spencer, T., Ferreira, O., Armaroli, C., McIvor, A., 2018. Historical analysis of storm events: case studies in France, England, Portugal and Italy. Coast. Eng. 134, 10–23. https://doi.org/10.1016/J.COASTALENG.2017.06.014.

Goldman Martone, R., Wasson, K., 2008. Impacts and interactions of multiple human perturbations in a California salt marsh. Oecologia 158, 151–163. https://doi.org/10.1007/s00442-008-1129-4.

Goslin, J., Bernatchez, P., Barnett, R.L., Béland, C., Ghaleb, B., Didier, D., Garneau, M., 2022. Importance of coarse sedimentation events in the resilience of microtidal back-

barrier saltmarshes to sea-level rise. Mar. Geol. 447, 106793 https://doi.org/10.1016/J.MARGEO.2022.106793.
Hein, C.J., Fenster, M.S., Gedan, K.B., Tabar, J.R., Hein, E.A., DeMunda, T., 2021. Leveraging the interdependencies between barrier islands and backbarrier saltmarshes to enhance resilience to sea-level rise. Front. Mar. Sci. 8, 1206. https://doi.org/10.3389/fmars.2021.721904.
Keizer, I., Le Bars, D., de Valk, C., Jüling, A., van de Wal, R., Drijfhout, S., 2023. The acceleration of sea-level rise along the coast of The Netherlands started in the 1960s. Ocean Sci. 19, 991–1007. https://doi.org/10.5194/os-19-991-2023.
Kirwan, M.L., Temmerman, S., Skeehan, E.E., Guntenspergen, G.R., Fagherazzi, S., 2016. Overestimation of marsh vulnerability to sea level rise. Nat. Clim. Change 63 (6), 253–260. https://doi.org/10.1038/nclimate2909, 2016.
Kombiadou, K., Costas, S., Carrasco, A.R., Plomaritis, T.A., Ferreira, Ó., Matias, A., 2019a. Bridging the gap between resilience and geomorphology of complex coastal systems. Earth Sci. Rev. 198, 102934 https://doi.org/10.1016/j.earscirev.2019.102934.
Kombiadou, K., Matias, A., Costas, S., Rita Carrasco, A., Plomaritis, T.A., Ferreira, Ó., 2020. Barrier island resilience assessment: applying the ecological principles to geomorphological data. Catena 194, 104755. https://doi.org/10.1016/j.catena.2020.104755.
Kombiadou, K., Matias, A., Ferreira, Ó., Carrasco, A.R., Costas, S., Plomaritis, T., 2019b. Impacts of human interventions on the evolution of the Ria Formosa barrier island system (S. Portugal). Geomorphology 343, 129–144. https://doi.org/10.1016/j.geomorph.2019.07.006.
Leuschner, C., Landwehr, S., Mehlig, U., 1998. Limitation of carbon assimilation of intertidal Zostera noltii and Z. marina by desiccation at low tide. Aquat. Bot. 62, 171–176. https://doi.org/10.1016/S0304-3770(98)00091-6.
Lobo, F.J., Hernández-Molina, F.J., Somoza, L., Díaz del Río, V., 2001. The sedimentary record of the post-glacial transgression on the Gulf of Cadiz continental shelf (Southwest Spain). Mar. Geol. 178, 171–195. https://doi.org/10.1016/S0025-3227(01)00176-1.
Lõhmus, K., Balke, T., Kleyer, M., 2020. Spatial and temporal patterns of initial plant establishment in salt marsh communities. J. Veg. Sci. 31, 1124–1134. https://doi.org/10.1111/jvs.12915.
Martins, M., de los Santos, C.B., Masqué, P., Carrasco, A.R., Veiga-Pires, C., Santos, R., 2022. Carbon and nitrogen stocks and burial rates in intertidal vegetated habitats of a mesotidal coastal lagoon. Ecosystems 25, 372–386. https://doi.org/10.1007/s10021-021-00660-6.
Matias, A., Ferreira, Ó., Vila-Concejo, A., Garcia, T., Dias, J.A., 2008. Classification of washover dynamics in barrier islands. Geomorphology 97, 655–674. https://doi.org/10.1016/j.geomorph.2007.09.010.
Morzaria-Luna, H.N., Zedler, J.B., 2007. Does seed availability limit plant establishment during salt marsh restoration? Estuar. Coast 30, 12–25. https://doi.org/10.1007/BF02782963.
Mudd, S.M., 2011. The life and death of salt marshes in response to anthropogenic disturbance of sediment supply. Geology 39, 511–512. https://doi.org/10.1130/FOCUS052011.1.
Neubauer, S.C., 2008. Contributions of mineral and organic components to tidal freshwater marsh accretion. Estuar. Coast Shelf Sci. 78, 78–88. https://doi.org/10.1016/J.ECSS.2007.11.011.
Neumeier, U., Ciavola, P., 2004. Flow resistance and associated sedimentary processes in a Spartina maritima salt-marsh. J. Coast Res. 20, 435–447. https://doi.org/10.2112/1551-5036(2004)020 [0435:FRAASP]2.0.CO;2.
Nielsen, N., Nielsen, J., 2002. Vertical growth of a young back barrier salt marsh, Skallingen, SW Denmark. J. Coast Res. 18, 287–299.
Ouyang, X., Connolly, R.M., Lee, S.Y., 2022. Revised global estimates of resilience to sea level rise for tidal marshes. Environ. Challenges 9, 100593. https://doi.org/10.1016/J.ENVC.2022.100593.
Pacheco, A., Ferreira, Ó., Williams, J.J., Garel, E., Vila-Concejo, A., Dias, J.A., 2010. Hydrodynamics and equilibrium of a multiple-inlet system. Mar. Geol. 274, 32–42. https://doi.org/10.1016/J.MARGEO.2010.03.003.
Pacheco, A., Monteiro, J., Santos, J., Sequeira, C., Nunes, J., 2022. Energy transition process and community engagement on geographic islands: the case of Culatra Island (Ria Formosa, Portugal). Renew. Energy 184, 700–711. https://doi.org/10.1016/J.RENENE.2021.11.115.
Pacheco, A., Williams, J.J., Ferreira, Ó., Garel, E., Reynolds, S., 2011. Applicability of sediment transport models to evaluate medium term evolution of tidal inlet systems. Estuar. Coast Shelf Sci. 95, 119–134. https://doi.org/10.1016/J.ECSS.2011.08.027.
Pedersen, J.B.T., Bartholdy, J., 2007. Exposed salt marsh morphodynamics: an example from the Danish Wadden Sea. Geomorphology 90, 115–125. https://doi.org/10.1016/J.GEOMORPH.2007.01.012.
Pethick, J.S., 1981. Long-term accretion rates on tidal salt marshes. J. Sediment. Res. 51, 571–577. https://doi.org/10.1306/212F7CDE-2B24-11D7-8648000102C1865D.
Pilkey, O.H.J., Neal, W.J., Virginia, C., 1989. Algarve barrier islands: a noncoastal-plain system in Portugal. J. Coast Res. 5, 239–261.
Pratolongo, P., Leonardi, N., Kirby, J.R., Plater, A., 2019. Temperate coastal wetlands: morphology, sediment processes, and plant communities. In: Perillo, G.M.E., Wolanski, E., Cahoon, D.R., Hopkinson, C.S. (Eds.), Coastal Wetlands: an Integrated Ecosystem Approach. Elsevier, pp. 105–152. https://doi.org/10.1016/B978-0-444-63893-9.00003-4.
Rodriguez, A.B., McKee, B.A., 2021. Salt marsh formation. In: FitzGerald, D.M., Hughes, Z.J. (Eds.), Salt Marshes. Cambridge University Press, pp. 31–52. https://doi.org/10.1017/9781316888933.004.
Rosa, A., Cardeira, S., Pereira, C., Rosa, M., Madureira, M., Rita, F., Jacob, J., Cravo, A., 2019. Temporal variability of the mass exchanges between the main inlet of Ria Formosa lagoon (southwestern Iberia) and the Atlantic Ocean. Estuar. Coast Shelf Sci. 228, 106349 https://doi.org/10.1016/J.ECSS.2019.106349.
Saintilan, N., Kovalenko, K.E., Guntenspergen, G., Rogers, K., Lynch, J.C., Cahoon, D.R., Lovelock, C.E., Friess, D.A., Ashe, E., Krauss, K.W., Cormier, N., Spencer, T., Adams, J., Raw, J., Ibanez, C., Scarton, F., Temmerman, S., Meire, P., Maris, T., Thorne, K., Brazner, J., Chmura, G.L., Bowron, T., Gamage, V.P., Cressman, K., Endris, C., Marconi, C., Marcum, P., St. Laurent, K., Reay, W., Raposa, K.B., Garwood, J.A., Khan, N., 2022. Constraints on the adjustment of tidal marshes to accelerating sea level rise. Science (80-.) 377, 523–527. https://doi.org/10.1126/science.abo7872.
Salles, P., Voulgaris, G., Aubrey, D.G., 2005. Contribution of nonlinear mechanisms in the persistence of multiple tidal inlet systems. Estuar. Coast Shelf Sci. 65, 475–491. https://doi.org/10.1016/J.ECSS.2005.06.018.
Schuerch, M., Dolch, T., Bisgwa, J., Vafeidis, A.T., 2018. Changing sediment dynamics of a mature backbarrier salt marsh in response to sea-level rise and storm events. Front. Mar. Sci. 5, 155. https://doi.org/10.3389/fmars.2018.00155.
Schuerch, M., Rapaglia, J., Liebetrau, V., Vafeidis, A., Reise, K., 2012. Salt marsh accretion and storm tide variation: an example from a barrier island in the North sea. Estuar. Coast 35, 486–500. https://doi.org/10.1007/s12237-011-9461-z.
Serpa, D., Jesus, D., Falcão, M., Cancela Da Fonseca, L., 2005. Ria Formosa Ecosystem: Socio-Economic Approach. Lisbon.
Silva, J., Santos, R., 2003. Daily variation patterns in seagrass photosynthesis along a vertical gradient. Mar. Ecol. Prog. Ser. Environ. Sci. 257, 37–44. https://doi.org/10.3354/MEPS257037.
Sousa, A.I., Santos, D.B., Silva, E.F. Da, Sousa, L.P., Cleary, D.F.R., Soares, A.M.V.M., Lillebø, A.I., 2017. "Blue carbon" and nutrient stocks of salt marshes at a temperate coastal lagoon (Ria de Aveiro, Portugal). Sci. Rep. 7, 1–11. https://doi.org/10.1038/srep41225.
Stoddart, D.R., Reed, D.J., French, J.R., 1989. Understanding salt-marsh accretion, scolt head island, Norfolk, England. Estuaries 12, 228. https://doi.org/10.2307/1351902.
Thieler, E.R., Himmelstoss, E.A., Zichichi, J.L., Ergul, A., 2009. The Digital Shoreline Analysis System (DSAS) Version 4.0—an ArcGIS Extension for Calculating Shoreline Change.
van Dobben, H.F., de Groot, A.V., Bakker, J.P., 2022. Salt marsh accretion with and without deep soil subsidence as a proxy for sea-level rise. Estuar. Coast 45, 1562–1582. https://doi.org/10.1007/s12237-021-01034-w.
Vila-Concejo, A., Matias, A., Ferreira, Ó., Duarte, C., Dias, J.M.A., 2002. Recent evolution of the natural inlets of a barrier island system in southern Portugal. J. Coast Res. 36, 741–752.
Walters, D., Moore, L.J., Duran Vinent, O., Fagherazzi, S., Mariotti, G., 2014. Interactions between barrier islands and backbarrier marshes affect island system response to sea level rise: insights from a coupled model. J. Geophys. Res. Earth Surf. 119, 2013–2031. https://doi.org/10.1002/2014jf003091.
Wolters, M., Garbutt, A., Bakker, J.P., 2005. Plant colonization after managed realignment: the relative importance of diaspore dispersal. J. Appl. Ecol. 42, 770–777. https://doi.org/10.1111/J.1365-2664.2005.01051.X.
Yando, E.S., Jones, S.F., James, W.R., Colombano, D.D., Montemayor, D.I., Nolte, S., Raw, J.L., Ziegler, S.L., Chen, L., Daffonchio, D., Fusi, M., Rogers, K., Sergienko, L., 2023. An integrative salt marsh conceptual framework for global comparisons. Limnol. Oceanogr. Lett. https://doi.org/10.1002/LOL2.10346.